

# Transforming Enhanced Landfill Mining Derived Gasification/Vitrification Glass into Low-Carbon Inorganic Polymer Binders and Building Products

Lieven Machiels<sup>1</sup> · Lukas Arnout<sup>1</sup> · Pengcheng Yan<sup>1</sup> · Peter Tom Jones<sup>1</sup> · Bart Blanpain<sup>1</sup> · Yiannis Pontikes<sup>1</sup>

© The Minerals, Metals & Materials Society (TMS) 2016

**Abstract** The current paper reviews the concept of the production of high-added value construction materials produced as part of a zero waste enhanced landfill mining process. The calorific fraction of the excavated waste is concentrated to produce a solid recovered fuel, which is introduced to a gasification/vitrification process to be converted to a synthetic gas, a slag and a metal alloy. The slag is subsequently cooled to produce a glass. The glass is milled and blended with an alkaline silicate solution to produce an inorganic polymer binder. The binder can be used as an alternative for ordinary Portland cement (OPC) in concrete to produce precast construction materials, such as pavers, tiles and wall elements. Pilot industrial production and testing of the durability, environmental footprint and economic feasibility of the process are currently being performed. Traditional OPC based production lines can be used, and when comparing with OPC based concrete, materials with similar to improved properties (e.g. higher hardening rate and higher final strength) can be produced.

**Keywords** Enhanced landfill mining · Plasma gasification · Solid recovered fuel · Vitrification · Inorganic polymer binders

## Introduction

Transition towards a resource efficient, low carbon circular economy is a necessity under the current conditions of climate change [1] and resource shortages [2]. As many sectors, the cement and construction industry is also subject to this transition. On a global scale, concrete, a mixture of cement, sand and gravel, is the second most consumed material after water, with the estimated production being 25 billion tonnes per annum [3]. It is estimated that 8% of world's total CO<sub>2</sub>-release results from cement production [3]. In the past, cement was almost exclusively made from clinker, produced as a mixture of limestone and clay, calcined at 1450 °C, ground and mixed with gypsum to form ordinary Portland cement (OPC). Although any material with binding capacities that hardens under ambient conditions can be termed cement, the market domination of OPC has led to the terms OPC and cement being used interchangeably. Today, however, the spectrum of cement types has broadened, due to the requirement for the sector to reduce greenhouse gas emissions, due to cost reduction and through the broad spectrum of properties required from construction materials. This is visible in several aspects: (1) secondary raw materials are being used as a source of energy and/or as raw materials for OPC clinker production [4]; (2) supplementary cementitious materials such as fly ash (from coal combustion) and ground granulated blast furnace slag (GGBFS, from steel production) are blended with OPC clinker to produce “blended cements” [4]; (3) alternative processes are used to produce binders free of OPC clinker. An example of a such a class of “alternative” binders are inorganic polymers (further abbreviated as IP's), commonly also termed “alkali activated materials” [5], or “geopolymers” [6, 7]. Commercially available “geopolymer cement” is most commonly composed of a

---

The contributing editor for this article was Dimitrios Panias.

---

✉ Lieven Machiels  
lieven.machiels@kuleuven.be

<sup>1</sup> Department of Materials Engineering, KU Leuven, Kasteelpark Arenberg 44, 3001 Heverlee, Belgium

mixture of fly ash, GGBFS and an alkaline silicate solution [8]. Alternative types are based on calcined kaolinitic clays [9]. “Geopolymer concretes” are being produced in Australia [8], India [10] and SouthAfrica [11], and have recently been introduced in the UK [9]. In Europe, an increasing amount of R&D is currently being performed in both industry and academia. In many niche applications, it can be stated that IP binders have found their entrance. Examples of the use of IP in existing commercial products are glues [12], sealing agents for sewage tubes [13] and binders in refractory moulds [14]. Large-scale industrial production of IP binders for general construction applications is expected in Europe within the next 5–10 years. This market introduction will result in an important rise in the demand of raw materials for IP production. As both the number of coal plants producing fly ash and iron blast furnaces producing GGBFS are declining in Europe, and as these plants are currently delivering the most important raw materials for IP binder production, the availability of alternative raw materials becomes an important issue.

### Production of Gasification/Vitrification Glass Within Enhanced Landfill Mining

An important class of alternative raw materials for IP production are glasses produced during the gasification/vitrification of calorific waste materials applied as fuels in the Waste-to-Energy sector. In Europe, gasification is an emerging technology considered as an important alternative for grate incineration of urban solid waste (USW) [15]. In many gasification flowsheets, gasification is associated with the vitrification of the inorganic ash fraction of the calorific materials and a vitreous material is thus produced, which could be a precursor for IP. The current paper focusses on glasses produced by the gasification/vitrification of secondary fuels generated during enhanced landfill mining (ELFM) [16]. Enhanced landfill mining has been defined as “the safe conditioning, excavation and integrated valorisation of landfilled waste streams as materials and energy, using innovative transformation technologies and respecting the most stringent social and ecological criteria” [17]. Existing and new landfills are thus considered as resource stocks awaiting future mining in order to recover valuable resources in an integrated way. While industrial landfills are commonly of economic interest for their metal value [17], the value of USW containing landfills lies mainly in the presence of high amounts of calorific materials, such as plastics, wood and textile. These highly calorific materials can be recycled, or, as recycling of these streams into their individual components is currently still very challenging, these materials can be concentrated to solid recovered fuels (further abbreviated

SRFs), that can be used as secondary resources for energy production. When looking at the huge amount of landfills throughout Europe (estimated between 150,000 and 500,000) [18], it is obvious that SRF produced by ELFM could have a large impact on SRF availability in Europe.

An example of an enhanced landfill mining flowsheet for USW-containing landfill involving thermal SRF conversion is shown in Fig. 1. Within this flowsheet, the current paper focusses on the production of glassy materials through the gasification/vitrification of SRF to a synthetic gas (further termed syngas), metal and glass and the subsequent “upcycling” of this glass to IP binders and high added value building products. The paper aims at summarizing the research performed by the authors in the period of 2011–2016 in both the pilot scale production of

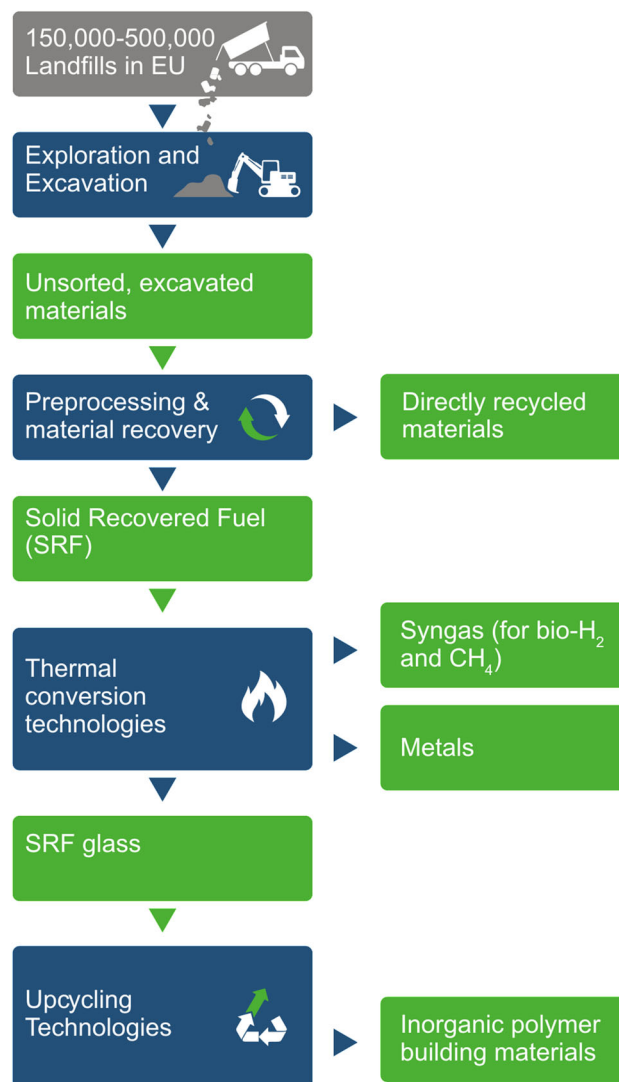


**Fig. 1** Inorganic polymer building materials production within an ELFM flowsheet

SRF glass and in its subsequent use in IP based building materials.

Two examples of gasification/vitrification setups for SRF conversion as used in ELFM are shown in Fig. 2. Although other set-ups are possible, a comparison of the suitability of different thermal conversion technologies for SRF derived from ELFM is out of scope of the current paper and has recently been published [15]. In the current paper, focus is on SRF gasification in combination with vitrification of the inorganic ash fraction of the SRF, as in the vitrification step an IP precursor can be produced. Gasification is defined as the partial oxidation of organic substances at elevated temperature (500–1800 °C) to produce a highly calorific synthesis gas (syngas), composed predominantly of H<sub>2</sub>, CO, CO<sub>2</sub>, H<sub>2</sub>O and CH<sub>4</sub>, when oxygen and steam are used as gasification agents. This gas can be either burned for combined heat and power production (CHP), or it can be used as a chemical feedstock to generate higher value products (e.g. H<sub>2</sub>, CH<sub>4</sub>, methanol). Vitrification refers to the melting of the inorganic ash fraction of the SRF to form a molten slag, which is subsequently tapped and rapidly cooled (granulated) to a glass, e.g. through quenching of the molten slag using water jets. As shown in Fig. 2, in industrial systems, SRF gasification is commonly decoupled in two stages, in which in the first step SRF is gasified to produce a crude syngas, while in a second step further “cleaning” of the gas is performed through cracking of remaining organic compounds in the gas, e.g. through the use of a high-temperature plasma and through capturing of solid particles, which is commonly done through a liquid slag bath. This gas cleaning step is required to ensure the gas to be of sufficient quality for use in high-added value applications, such as the production of hydrogen.

Depending on the type of process that is used to produce the glassy phase, different names have been given to the

glasses, e.g. “Plasmarok<sup>®</sup>” [19], “plasmastone” [20], “plasma convertor slag” [21], “residue of DC plasma treatment” [22–24], “inert slag” [25], waste gasification/vitrification slag [26]. In the current paper, the term SRF-glass is used, referring to a glass resulting from the gasification/vitrification of SRF. The term “SRF-glass” is used rather than “glass”, to distinguish from the glass cullets (bottles glass, window glass, etc.) that is commonly recovered during the pre-processing and material recovery from USW in an ELFM flowsheet [27] (Fig. 1). The research performed on SRF glasses at KU Leuven [20, 21, 28–30] is summarized in the current paper, covering both the “hot stage engineering” of the glass in the SRF gasification/vitrification process and the subsequent inorganic polymerisation of the glass. Other authors have studied the inorganic polymerisation of raw materials of comparable chemistry, such as glasses resulting from the plasma vitrification of air pollution control residues [22–24] and glasses resulting from the plasma vitrification of grate incinerator bottom ash [31].

### SRF-Glass Compositional Variation

To evaluate the suitability of using SRF-glass as a precursor for IP binder production, in a first step, a prediction of the composition and of the compositional variation of the glass chemistry is made. This chemistry is determined by the chemistry of the inorganic ash fraction of the SRF fed to the gasification/vitrification process. SRF chemistry is expected to vary widely depending on the source material (USW or industrial waste—IW), geographical origin, age (fresh waste or landfilled waste) and applied pre-concentration method. To have an idea about this compositional variation, analyses of freshly produced SRF were collected from literature [32]. To broaden the data set,

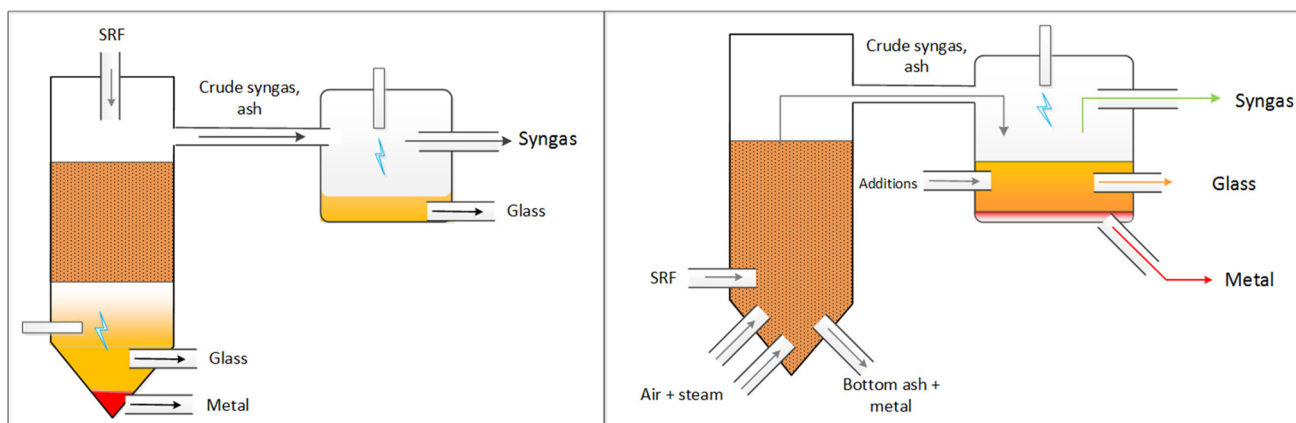


**Fig. 2** High temperature gasification/vitrification unit for syngas, glass and metal production from SRF. *Left* 2-stage system with majority of glass + metal formed in the first stage. *Right* 2-stage

system with bottom ash formation in the first-low-T-stage and glass + metal formation in the second stage

compositional data of USW grate incinerator bottom ashes were also consulted, as their chemistry is expected to be similar to SRF chemistry [31, 33]. SRF analyses from ELFM were sourced from research performed by the authors in a landfill containing both USW and IW [34]. Results are shown in Table 1 and Fig. 3. Contents of C and H of the ash are omitted, as these elements end up in the gas phase during gasification/vitrification, while only traces of these elements remain in the glass. A comparison is made to the chemistry of commonly used raw materials for IP binder production.

When looking at Fig. 3, it can be observed that most SRF-samples have a chemistry close to GGBFS and Carich fly ash (termed class C fly ash), indicating a promising chemistry for use as raw materials for IP binders. When looking at the SRF ash samples from ELFM, a similar chemistry is observed. Notable is the high Fe content of some of the ELFM samples, which can probably be attributed to their IW origin.

### High Temperature Modelling of Slag Making in the Gasification/Vitrification Process

With the compositional variation of the SRF ash known, the possibility of producing a glass through SRF gasification/vitrification is reviewed. High temperature modelling is used to predict the melt characteristics, such as melting temperature and viscosity, allowing the production of a workable slag that can be tapped and cooled to produce a glass. Details of the model development and model parameters can be found in Yan et al. [30] as well as in Arnout and Nagels [36]. As an example, a calculation of the characteristics of three slag types produced from SRF

derived from ELFM is performed. One SRF is derived from excavated and pre-processed USW (no. 5 in Fig. 3), another from excavated and pre-processed IW (no. 4 in Fig. 3) and a third one is a 50:50 blend of the two SRF types (no. 6 in Fig. 3). Ashed SRF compositions are given in Table 2. SRF is gasified under an oxygen/steam atmosphere at 1400 °C to form a syngas, a slag and a metal phase, as schematically represented in Fig. 4. Oxygen and steam content are adjusted to reach a syngas of oxygen partial pressure of  $10^{-8}$  atm (determined by the  $(\text{CO} + \text{H}_2 + \text{CH}_4)/(\text{CO}_2 + \text{H}_2\text{O})$  content). Thermodynamic equilibrium between the syngas and slag phases is assumed. In the IW and blended systems, a separate metallic phase is formed, but compared to the slag phase, the amount of metal is limited (metal/slag ratios of 1.7 and 0.7 to 100 respectively). The calculated slag melting temperature and viscosity of the resulting slags are given in Table 3 and the composition of the slag and metal phases are given in Tables 4 and 5. When looking at the melting temperatures in Table 3, all slags are fully liquid at 1400 °C. When looking at the viscosity, the viscosity of the USW slag is determined to be  $15 \times$  higher than of the IW slag, which could deliver problems for the tapping of the slag. This could be resolved through (1) heating the slag to a higher temperature; (2) blending of the USW and IW SRF hereby reaching a blend composition of reduced viscosity; (3) addition of CaO to the mixture to direct the USW composition to the lower viscosity region.

When comparing the SRF ash and glass compositions in Tables 4 and 5, it is observed that these are rather similar for most elements. Differences exist in the  $\text{Fe}^{2+}/\text{Fe}^{3+}$  ratio, expressed as FeO and  $\text{Fe}_2\text{O}_3$ , and the contents of heavy elements such as Pb, Zn, Cu, Ni. Both parameters depend on the composition and oxidation state of these elements in the feed materials, the composition of the syngas (reducing power of the syngas determined by the  $(\text{H}_2 + \text{CO} + \text{CH}_4)/(\text{CO}_2 + \text{H}_2\text{O})$  ratio) and the degree of slag/syngas interaction in the gasification/vitrification process. The latter is determined by the reducing power of the syngas and the extent to which the syngas is able to interact and equilibrate with the slag, which is again dependent on the process conditions, geometry of the furnace and slag residence time. A higher degree of slag reduction will lead to a higher  $\text{Fe}^{2+}/\text{Fe}^{3+}$  ratio and a reduced content of heavy metals in the slag, as these will be separated in the metallic phase (Cu, Ni) or the gas phase (Pb, Zn). This is especially important for SRF derived from industrial waste, as these tend to contain higher metal content. The results presented here assume full gas/slag equilibrium and thus indicate the maximum possible slag reduction for the given syngas composition. In industrial systems however, complete gas/slag equilibrium is not necessarily attained. Models have been developed using partial syngas/slag equilibrium,

**Table 1** SRF ash compositional range compared to GGBFS and fly ash compositional range (in wt%)

|                         | SRF ash<br>Median | Range | GGBFS [35] | Fly ash [35] |
|-------------------------|-------------------|-------|------------|--------------|
| $\text{Al}_2\text{O}_3$ | 12                | 4–22  | 5–15       | 5–35         |
| CaO                     | 22                | 15–39 | 30–50      | 1–40         |
| $\text{SiO}_2$          | 39                | 22–62 | 27–40      | 15–60        |
| $\text{Fe}_2\text{O}_3$ | 11                | 1–9   | 0–1        | 4–40         |
| MgO                     | 2                 | 0–6   | 1–10       | –            |
| $\text{SO}_3$           | 3                 | 0–7   | 0–5        | –            |
| $\text{Na}_2\text{O}$   | 3                 | 0–6   | –          | –            |
| Cl                      | 2                 | 0–3   | –          | –            |
| $\text{K}_2\text{O}$    | 1                 | 0–4   | –          | –            |
| $\text{P}_2\text{O}_5$  | 1                 | 0–5   | –          | –            |
| $\text{TiO}_2$          | 2                 | 0–5   | –          | –            |
| Others                  | 1                 | 0–13  | –          | –            |

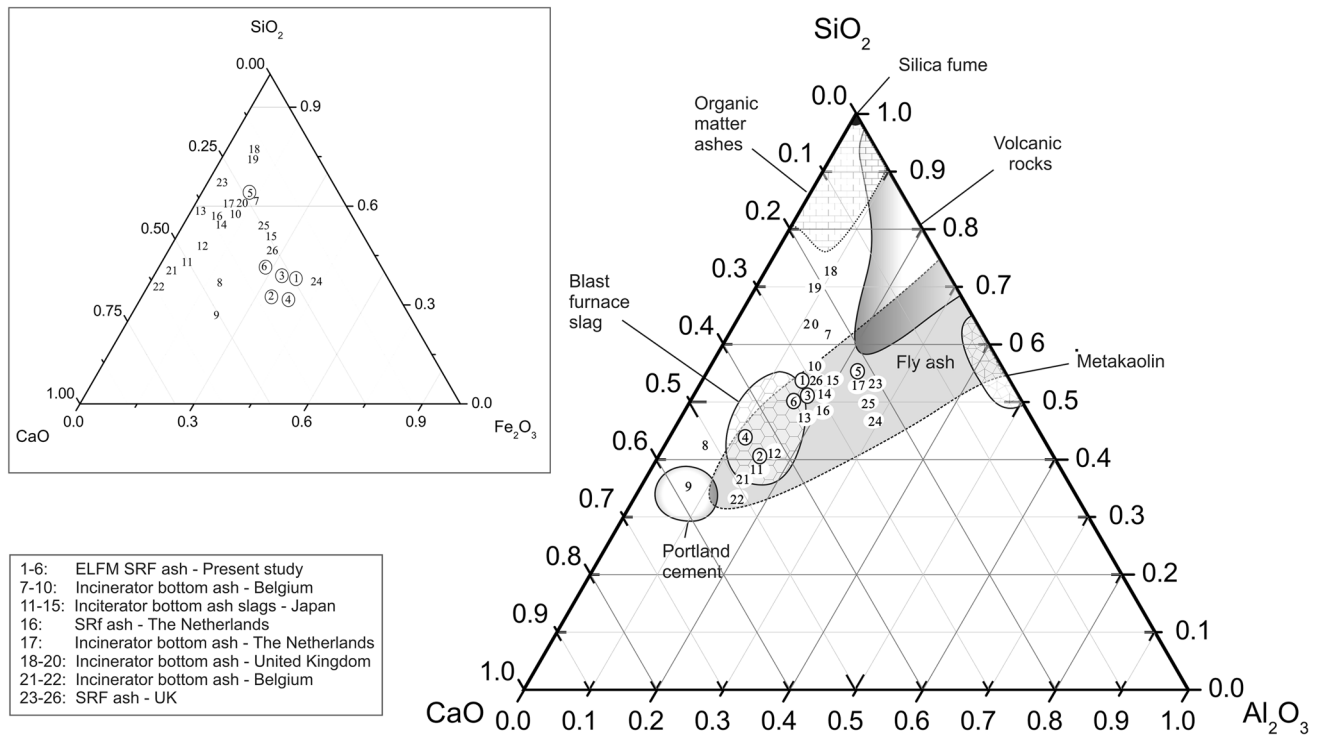


**Fig. 3** Compositional variation of ELFM derived SRF ash, SRF ash from fresh USW and grate incinerator bottom ash

**Table 2** Analyses of SRF from ELFM

| Wt%                            | IW-SRF | USW-SRF | Blend |
|--------------------------------|--------|---------|-------|
| Al <sub>2</sub> O <sub>3</sub> | 6.3    | 17.0    | 11.7  |
| CaO                            | 24.9   | 17.7    | 21.3  |
| CuO                            | 2.0    | 0.1     | 1.1   |
| Fe <sub>2</sub> O <sub>3</sub> | 27.3   | 11.8    | 19.6  |
| K <sub>2</sub> O               | 0.4    | 1.3     | 0.9   |
| MgO                            | 3.8    | 3.0     | 3.4   |
| Na <sub>2</sub> O              | 3.9    | 4.0     | 3.9   |
| NiO                            | 0.2    | 0.1     | 0.1   |
| SiO <sub>2</sub>               | 24.5   | 41.6    | 33.0  |
| TiO <sub>2</sub>               | 1.6    | 1.6     | 1.6   |
| ZnO                            | 3.2    | 0.5     | 1.8   |
| Cr <sub>2</sub> O <sub>3</sub> | 0.2    | 0.3     | 0.2   |

IW industrial waste, USW urban solid waste, Blend blend of IW and USW SRF

resulting in lower Fe<sup>2+</sup>/Fe<sup>3+</sup> ratios in the slag and higher residual heavy metal content [30]. Tests in full-scale industrial systems are needed to indicate the degree of gas/slag interaction and thus the eventual Fe oxidation state and heavy metal content in the slags. Depending on the economics of the process, decision on the required degree of gas/slag interaction can be made. If gas is the main output product of the process (and this is commonly the case, as

confirmed by the mass balance in Fig. 4), it can be preferred to limit gas/slag interaction, as oxidation of the syngas would lead to a lower syngas quality. However in certain industrial SRF types, where valuable metals could be recovered, gas/slag interaction could be enhanced to increase the degree of reduction and thus recover these metals.

### SRF-Glass Production

Glass production was performed on both small scale, in the lab, and on large scale, in a pilot industrial scale vitrification unit. Lab-scale production was performed to evaluate the high temperature modelling results and to produce glass samples for IP production. Glasses of varying characteristics (e.g. chemistry or crystalline content) were produced to evaluate the effect of varying glass characteristics on IP properties. Syngas reduction of the slag was mimicked through equilibration with a CO/CO<sub>2</sub> gas mixture (see Fig. 5), to ensure Fe being present predominantly as Fe<sup>2+</sup>, as would be the case under syngas/slag equilibrium. Immediate quenching of the molten slag to a glass was done on lab scale through dipping a steel bar in the slag and quenching the bar in water (Fig. 5). Pilot scale production of glass was performed to upscale the lab-scale results and to produce sufficient glass to perform pilot testing of the IP binder production. Due to the limited

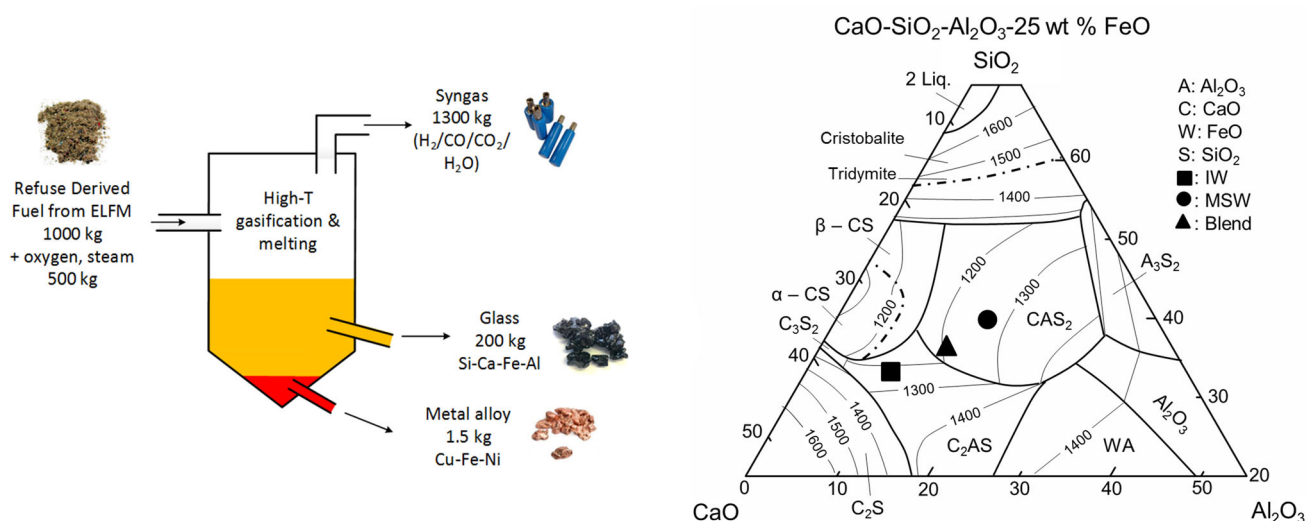


**Fig. 4** *Left* Schematic representation of a high temperature gasification and melting system for SRF conversion. *Right* Phase diagram indicating melt compositions of SRF ash from IW (sample 4 in Fig. 3), USW (sample 5 in Fig. 3) and a blend of both SRF types (sample 6 in Fig. 3)

**Table 3** Melting T and Viscosity of SRF derived glasses

|                                | IW-SRF | USW-SRF | Blend |
|--------------------------------|--------|---------|-------|
| Melting T (°C)                 | 1277   | 1347    | 1323  |
| Viscosity at 1400 °C (mP a. s) | 100    | 1500    | 300   |

**Table 4** Glass compositions derived from SRF in Table 2

| wt%                            | IW-SRF | USW-SRF | Blend |
|--------------------------------|--------|---------|-------|
| Al <sub>2</sub> O <sub>3</sub> | 6.7    | 17.3    | 12.1  |
| CaO                            | 26.6   | 18.0    | 22.2  |
| Cu <sub>2</sub> O              | 0.5    | 0.1     | 0.4   |
| FeO                            | 27.3   | 11.9    | 20.0  |
| Fe <sub>2</sub> O <sub>3</sub> | 2.0    | <0.1    | 0.5   |
| K <sub>2</sub> O               | 0.4    | 1.3     | 0.9   |
| MgO                            | 4.0    | 3.0     | 3.5   |
| Na <sub>2</sub> O              | 4.2    | 4.0     | 4.1   |
| NiO                            | <0.1   | <0.1    | <0.1  |
| SiO <sub>2</sub>               | 26.2   | 42.2    | 34.3  |
| TiO <sub>2</sub>               | 1.7    | 1.6     | 1.7   |
| ZnO                            | <0.1   | 0.0     | 0.0   |
| Cr <sub>2</sub> O <sub>3</sub> | 0.1    | <0.1    | 0.1   |

capacity of the pilot set-up and in order to limit the pilot trial time, USW bottom ash (sample 10 on Fig. 2) was used as a source material for glass production rather than SRF. Indeed, to produce 1 tonne of ash from an SRF of 15% ash content ~7 tonnes of SRF would have to be treated and ~13 tonnes of syngas would be produced and this would

**Table 5** Composition of the metallic phase

| wt% | IW-SRF | USW-SRF | Blend |
|-----|--------|---------|-------|
| Cu  | 87.9   | N/A     | 88.0  |
| Fe  | 7.0    |         | 4.8   |
| Ni  | 4.9    |         | 7.0   |

unnecessarily complicate the pilot test. Additions of iron ore, limestone and sand were performed to adjust the ash chemistry to a composition similar to composition 6 in Fig. 3 (the blended SRF derived USW/IW sample in Table 2). To ensure that a glassy phase was produced, water jets and a water tank were used to quench the liquid slag (see Fig. 5). The bulk composition measured by XRF of the glass produced is given in Table 6. QXRD analysis of the glass phase indicates that the material is nearly entirely glassy, with crystalline phases limited to <2 wt% magnetite. Droplets of a metallic alloy rich in Cu can be observed as a separate phase within the glass (Fig. 5), as was predicted in the high temperature modelling.

### Inorganic Polymer Binder from SRF-Glass

Research has been performed on the inorganic polymerisation of SRF glass by the authors, results have been partially published already in previous publications. Investigation covered the following areas: (1) The influence of slag cooling rate on the crystalline/glass assemblage in the SRF-glass and on the glass reactivity in IP mixtures [28]; (2) Mix design of the IP binder, i.e. dosing of activator and composition of the activator (X<sub>2</sub>O/SiO<sub>2</sub>/H<sub>2</sub>O, with X being Na or K and influence of these



**Fig. 5** Upper left Lab-scale set-up for glass production; upper right Pilot scale set-up for glass production. Lower left Glass produced on lab-scale. Lower center glass produced on pilot scale; lower right

Backscattered electron microscopy image of milled glass particles containing spherical Cu-alloy droplets

**Table 6** Glass composition produced during the pilot trial

| SiO <sub>2</sub> | FeO   | CaO   | Al <sub>2</sub> O <sub>3</sub> | MgO  | Na <sub>2</sub> O | TiO <sub>2</sub> | K <sub>2</sub> O | CuO  | Cr <sub>2</sub> O <sub>3</sub> | ZnO  | NiO  | Oth. |
|------------------|-------|-------|--------------------------------|------|-------------------|------------------|------------------|------|--------------------------------|------|------|------|
| 35.00            | 21.00 | 23.00 | 16.00                          | 2.00 | 0.70              | 1.00             | 0.50             | 0.50 | 0.20                           | 0.02 | 0.08 | 0.80 |

parameters on IP microstructure and properties [21, 29]; (3) Influence of the glass chemistry on glass reactivity and IP properties, e.g. Fe<sup>2+</sup>/Fe<sup>3+</sup> substitution in the glass [37] or Ca/K/Na substitution in the glass [38]; (3) Heavy metal immobilisation/availability in glass-based IP's [39]. This abovementioned research has led to the development of an IP binder that can be used as an alternative for OPC cement in concrete and that can be applied in general construction applications, such as for the production of pavers, tiles, walls elements, etc. To illustrate the concept of IP binder production from SRF glass, an IP mortar was produced on lab-scale from the SRF glass produced on pilot scale in the previous section (glass composition in Table 6). The concept of producing the IP concrete is shown schematically in Fig. 6.

To prepare the mortar, SRF-glass was dried at 60 °C and milled in an attritor mill to a Blaine fineness of 5800 g/cm<sup>2</sup> (EN196-6). A two-component IP binder was prepared with the milled glass and an activating solution of composition in wt% SiO<sub>2</sub>: 19.5; K<sub>2</sub>O: 19.5; H<sub>2</sub>O: 61. The activator was

prepared by adjusting a commercial K-silicate solution (Woellner Betol K35T) of molar SiO<sub>2</sub>/K<sub>2</sub>O ratio 3.43 to a ratio of 1.6 through addition of KOH solution. Inorganic polymer mortars were prepared using a standard Hobart laboratory mixer through mixing the glass powder, the activator and sand aggregates. As aggregates, norm CEN sand (EN 196-1) was used. A castable mixture was produced that was casted in standard 4 × 4 × 16 cm<sup>3</sup> steel moulds and cured wrapped in plastic foil at 20 °C till mechanical testing. Mix proportions of glass, activating solution and sand aggregates are given in Table 7 (Formulation 1). Three-point bending tests and compressive strength tests were performed according to EN 196-1. Results are shown in Fig. 7. Results indicate a high early strength (compressive strength of 40 MPa at 2 days) and final strength (compressive strength of 140 MPa at 98 days and tree point-bending strength 13 MPa) and thus indicate that use as replacement of OPC in general and even high performance concrete can be considered. It has to be noted that it was aimed to demonstrate the maximal potential of

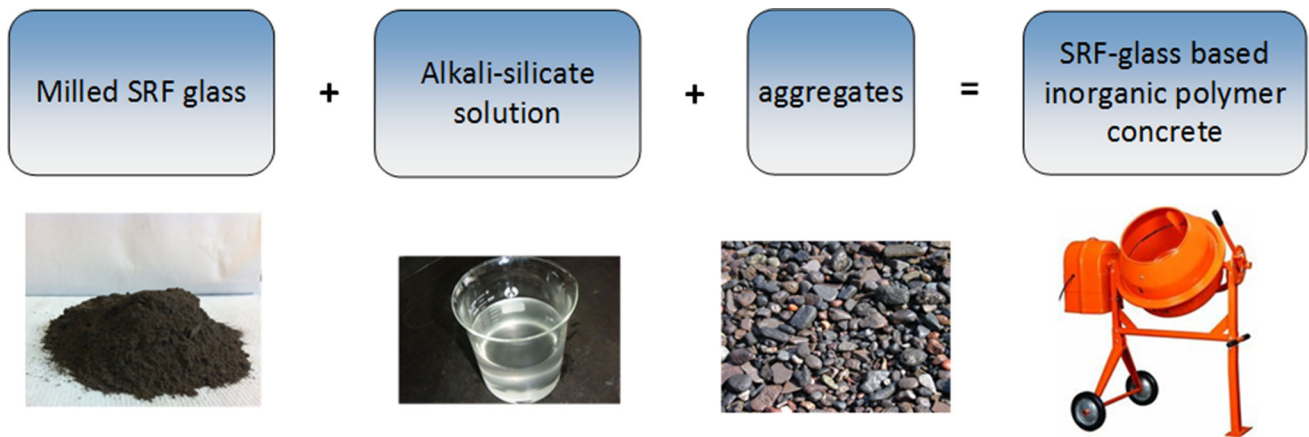


**Fig. 6** SRF-glass inorganic polymer concrete

**Table 7** Mix proportions of SRF-glass inorganic polymer mortar

| wt%           | SRF glass | Activator (dry basis) | Water | CEN sand |
|---------------|-----------|-----------------------|-------|----------|
| Formulation 1 | 26        | 4                     | 6     | 64       |
| Formulation 2 | 26        | 3                     | 7     | 64       |

As activator K-silicate of molar ratio of  $\text{SiO}_2/\text{K}_2\text{O}$  1.6 is used. Water refers to water present the activator + additional water added to the mixture

Formulation 2 is an optimized formulation allowing reduction of early-age cracking in the mixture

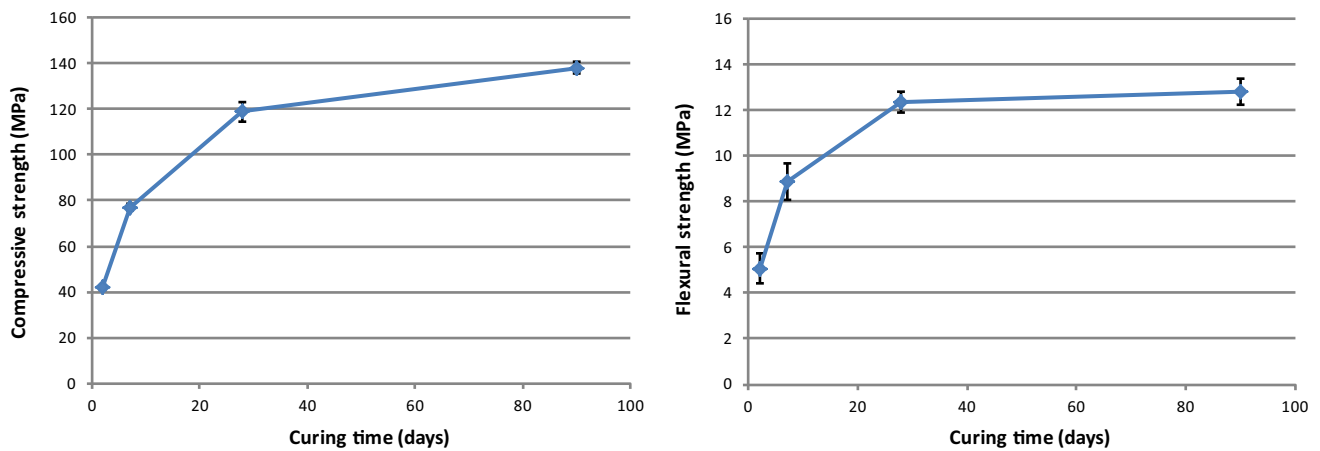


**Fig. 7** Results of compressive strength and 3-point bending strength development of SRF-based inorganic polymer mortars hardened at 20 °C

the binder system, especially with regards to early strength, as fast hardening is of high importance in the pre-cast sector to limit the curing and thus factory time. For other applications, such as ready mixed concrete, lower activator dosages can be considered as it is mostly not necessary to have such a high rates of strength development. Additionally, when scaling up, larger volumes of concrete will cool down much more slowly in comparison to the low volumes produced in the lab, hereby increasing reaction kinetics. Less activator is thus needed on industrial scale. Further optimisation of the mix design is currently being performed to use the material on industrial scale in a wide

variety of construction materials, such as pavement stones, tiles, precast concrete wall elements, etc.

### Proof of Concept: Pilot Scale Production of Pavement Stones Using SRF Glass-Based Inorganic Polymer as a Binder

To evaluate the performance of the SRF-based IP binder in a real-life industrial production environment, a pilot industrial test of paver production was performed in which the OPC binder normally used was replaced by the SRF-

glass based IP binder. 500 kg of SRF-glass were produced on pilot scale, of the composition indicated in Table 6. The mix design given in Table 7 was adjusted to develop a mix that could be used in a dry cast pressing production system. CEN sand—used for lab-scale IP production was replaced by the aggregate mix currently used in the industrial paver production. Mixture consistency was adapted to produce a dry mix by proportioning the activator, water and SRF-glass content and coarse and fine aggregates in the aggregate mix. Two square meters of pavers were produced (Fig. 8) and were cured together with the OPC based pavers under ambient conditions stacked in open racks in the production hall, without control of temperature or ambient humidity. Temperature was estimated to be around 20 °C. Properties were compared with original OPC based pavers. Compressive strength was measured on  $4 \times 4 \times 4 \text{ cm}^3$  cubes cut from the pavers, about 5 months after the production. Compressive strength analysis indicates no differences in strength between the SRF-glass and OPC pavers, with compressive strength being  $47.5 \pm 5.6 \text{ MPa}$  (Table 8).

### Current Work: Reducing Activator Content and Shrinkage Cracking in SRF-Based IP Binders

Currently pilot industrial tests are in progress to evaluate the SRF-glass binder in other precast applications, such as tiles and wall elements. Performance and durability of the materials will be tested and communicated in future publications. Life cycle and life cost analysis have been performed for the overall ELFM concept and for the production and use of glasses produced in the gasification/vitrification of SRF in ELFM. When looking at the production of traditional geopolymer cement, based on GGBFS and fly ash, the alkaline activator is the main

contributor to both the cost of the binder as for the environmental impact [5]. A similar observation was made for IP binders produced from SRF-glass [20]. Although the activator content in the binder mix (dry weight basis) given in Table 7 of 13 wt% is already low, it is obvious that for most applications the high early and late strength as given in Fig. 7 is not required and reduction of the activator content can be considered. In this way, the IP also becomes price competitive with OPC. In commercial fly ash—GGBFS systems, activator contents up to 3–5 wt% have been reported, resulting in a compressive strength of about 30 MPa at 28 days [8]. Additionally, replacement of the K-based activator by a Na-based activator is currently also being tested, and this also greatly reduces the cost. An important additional advantage in lowering the activator content is the reduction of shrinkage cracking [29]. In contrast to Portland cement, where shrinkage and cracking is a phenomenon occurring mainly in the later curing and drying stage, in glass based IP, shrinkage—and associated cracking of the binder—can occur in an early stage of hardening—e.g. within the first 24 h, when water is expelled from the network during polymerisation reactions [40]. An example of shrinkage cracks can be seen in Fig. 9, showing the microstructure of the IP mortar sample produced in the lab with the formulations given in Table 7—Formulation 1. Research in progress indicates that when part of the activator in a binder mix is replaced by water (Formulation 2 in Table 7), a strong reduction of shrinkage cracking can be obtained. A similar reduction in cracking is observed when an activator of the  $\text{SiO}_2/\text{K}_2\text{O}$  ratio of the activator is increased (in the current pilot tests, an activator of molar  $\text{SiO}_2/\text{K}_2\text{O}$  ratio of 2.0 is used). Research is in progress to obtain a full understanding of the mechanisms of shrinkage and micro-cracking in the IPs. Both dilution of the activator and increasing the  $\text{SiO}_2/\text{K}_2\text{O}$  ratio of the activator result in slower dissolution and

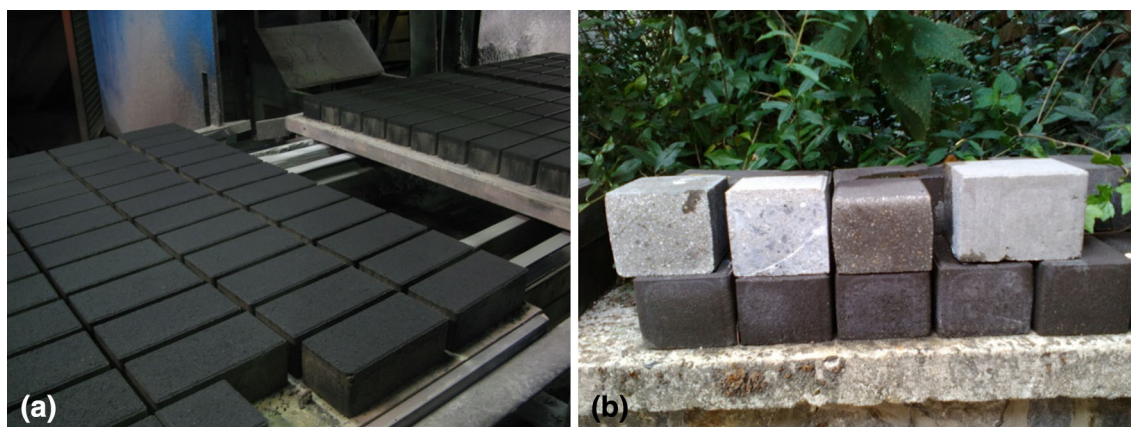


**Fig. 8** **a** Production of first batch of industrially produced pavers in which Portland cement has been fully replaced by SRF-glass inorganic polymer binder. **b** Comparison of Portland cement (*light color*) and SRF-glass based inorganic polymer binder pavers (*dark color*)

**Table 8** Compressive strength values of pavers

| Sample                            | Compressive strength (MPa) | Standard deviation (MPa) |
|-----------------------------------|----------------------------|--------------------------|
| SRF-glass inorganic polymer paver | 47.5                       | 5.6                      |
| Portland cement paver             | 43.2                       | 7.1                      |

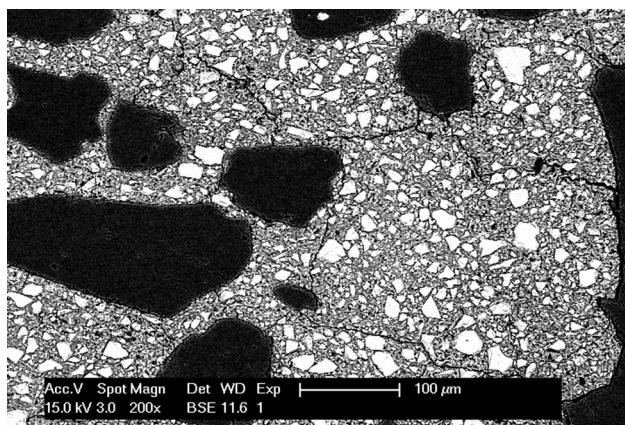


**Fig. 9** Image (SEM-BSE) of the inorganic polymer mortar produced on lab-scale (mix design Table 6). Large dark grains are CEN sand aggregates, white grains are partially dissolved SRF-glass. Inorganic polymer binder is grey in color. Black shrinkage cracks can be observed. Current research indicates that these cracks can be reduced by adjusting the water content of the activator or by increasing the  $\text{SiO}_2/\text{Na}_2\text{O}$  ratio of the activator

polymerisation kinetics, lower initial heat release and slower setting and hardening of the IP network. In IP mixtures with these reduced reaction kinetics, macro-cracks can be completely eliminated. More detailed results will be communicated in a future publication.

## Conclusions

The current paper explicates the potential of producing an inorganic polymer binder from SRF-glass, a by-product of SRF gasification/vitrification for syngas production from highly calorific waste materials. The binder can be used as an alternative for OPC in concrete and pre-cast applications, but can also be designed for novel high-added value applications, e.g. requiring high early strength (40 MPa at 2 days) or final strength (140 MPa at 90 days). First pilot industrial tests of the binder for precast paver production have shown that a full replacement of OPC by the novel binder system without important adaptations to the current industrial production lines is feasible. Continued testing is currently being performed for other applications such as tiles and wall elements.

**Acknowledgements** We gratefully acknowledge the Agentschap voor Innovatie door Wetenschap en Technologie (IWT), Milieu- en energietechnologie Innovatie Platform (MIP), i-CleanTech Vlaanderen, Groep

Machiels and the partners in the Closing the Circle and PLASMAT projects.

## References

1. Rockström J, Steffen W, Noone K et al (2009) Planetary boundaries: exploring the safe operating space for humanity. *Ecol Soc* 14:472–475
2. European Commission (2014) Report on critical raw materials for the EU: report of the Ad hoc Working Group on defining critical raw materials. <http://ec.europa.eu/DocsRoom/documents/10010/attachments/1/translations/en/renditions/native>. Accessed 30 June 2016
3. Provis JL (2014) Green concrete or red herring? Future of alkali-activated materials. *Adv Appl Ceram* 113:472–477
4. Snellings R, Mertens G, Elsen J (2012) Supplementary cementitious materials. *Rev Miner Geochem* 74:211–278. doi:10.2138/rmg.2012.74.6
5. Provis JL, Van Deventer JSJ (2014) Alkali activated materials. Springer, London
6. Davidovits J (2011) Geopolymer chemistry and applications, 3rd edn. Institut Géopolymère, Saint-Quentin
7. Provis LJ, van Deventer JSJ (2009) Geopolymers: structures, properties and industrial processing applications. Woodhead Publishing, Cambridge
8. Zeng D, Van Deventer JSJ, Duxson P (2007) Dry mix cement composition, methods and systems involving same. Patent WO 2007109862 A1
9. Banah UK (2015) High performance geopolymer cement. <http://www.banahuk.co.uk/>. Accessed 30 June 2016
10. Rajamane NP, Nataraja MC, Jeyalakshmi R, Nithiyanantham S (2015) Greener durable concretes through geopolymerisation of blast furnace slag. *Mater Res Express*. doi:10.1088/2053-1591/2/5/055502
11. Attwell C (2014) Geopolymer concrete: a practical approach. In: Proceedings of the first international conference on construction materials and structures, pp 466–474
12. PCI Geofug® - The high-convenience geopolymer joint grout that is almost self-cleaning. <https://www.pci.ch/produkte/pci-geofug/>. Accessed 30 June 2016
13. Introducing Bluey's new Geopolymer range. In: 14/7/2015. <http://www.bluey.com.au/civil-engineering-blog/technology/introducing-blueys-new-geopolymer-range>. Accessed 30 June 2016
14. GEOPOL® The environmental binder process for a sustainable future. <http://www.sandteam.cz/en/geopol-the-environmental-binder-process-for-a-sustainable-future/>. Accessed 30 June 2016
15. Bosmans A, Vanderreydt I, Geysen D, Helsen L (2013) The crucial role of Waste-to-Energy technologies in enhanced landfill mining: a technology review. *J Clean Prod* 55:10–23
16. Jones PT, Geysen D, Tielemans Y et al (2013) Enhanced Landfill Mining in view of multiple resource recovery: a critical review. *J Clean Prod* 55:45–55
17. Binnemans K, Jones PT, Blanpain B et al (2015) Towards zero-waste valorisation of rare-earth-containing industrial process residues: a critical review. *J Clean Prod* 99:17–38
18. Van Passel S, Dubois M, Eyckmans J et al (2013) The economics of enhanced landfill mining: private and societal performance drivers. *J Clean Prod* 55:92–102

19. Taylor R, Ray R, Chapman C (2013) Advanced thermal treatment of auto shredder residue and refuse derived fuel. *Fuel* 106:401–409
20. Danthurebandara M, Van Passel S, Machiels L, Van Acker K (2015) Valorization of thermal treatment residues in enhanced landfill mining: environmental and economic evaluation. *J Clean Prod* 99:275–285
21. Kriskova L, Machiels L, Pontikes Y (2015) Inorganic polymers from a plasma convertor slag: effect of activating solution on microstructure and properties. *J Sustain Metall* 1:240–251
22. Kourti I, Rani DA, Deegan D et al (2010) Production of geopolymers using glass produced from DC plasma treatment of air pollution control (APC) residues. *J Hazard Mater* 176:704–709
23. Kourti I, Rani DA, Boccaccinia R, Cheeseman CR (2011) Geopolymers from DC plasma-treated air pollution control residues, metakaolin, and granulated blast furnace slag. *J Mater Civ Eng* 23:735–740
24. Kourti I, Devaraj AR, Guerrero Bustos A et al (2011) Geopolymers prepared from DC plasma treated air pollution control (APC) residues glass: properties and characterisation of the binder phase. *J Hazard Mater* 196:86–92
25. Moustakas K, Fatta D, Malamis S et al (2005) Demonstration plasma gasification/vitrification system for effective hazardous waste treatment. *J Hazard Mater* 123:120–126
26. Byun Y, Namkung W, Cho M et al (2010) Demonstration of thermal plasma gasification/vitrification for municipal solid waste treatment. *Environ Sci Technol* 44:6680–6684
27. Quaghebeur M, Laenen B, Geysen D et al (2013) Characterization of landfilled materials: screening of the enhanced landfill mining potential. *J Clean Prod* 55:72–83
28. Pontikes Y, Machiels L, Onisei S et al (2013) Slags with a high Al and Fe content as precursors for inorganic polymers. *Appl Clay Sci* 73:93–102
29. Machiels L, Arnout L, Jones PT et al (2014) Inorganic polymer cement from Fe-silicate glasses: varying the activating solution to glass ratio. *Waste Biomass Valoriz* 5:411–428
30. Yan P, Pandelaers L, Machiels L et al (2015) Effect of gas–slag interaction on valorisation of refuse derived fuel treated with plasma gasification. *Min Process Extr Metall* 124:76–82
31. Yamaguchi N, Nagaishi M, Kisu K et al (2013) Preparation of monolithic geopolymer materials from urban waste incineration slags. *J Ceram Soc J* 121:847–854
32. ECN Phyllis 2 database for biomass and waste (2012). <https://www.ecn.nl/phyllis2/>. Accessed 30 June 2016
33. De Boom A, Degrez M (2012) Belgian MSWI fly ashes and APC residues: a characterisation study. *Waste Manag* 32:1163–1170
34. Spooen J, Quaghebeur M, Nielsen P, et al (2013). Material recovery and upcycling within the elfm concept of the Remo case. In: Proceedings of 2nd international academic symposium on enhanced landfill mining, Houthalen-Helchteren, pp 131–156
35. Taylor HFW (1997) *Cement chemistry*, 2nd edn. Thomas Telford Publishing, London
36. Nagels E, Arnout S (2016) The use of flowsheet modelling for feasibility assessment of novel waste treatment methods. In: Proceedings of 3rd international enhancement landfill mining symposium, Lisbon, Portugal, pp 277–287
37. Machiels L, Arnout L, Nagels E, et al (2015) Properties of inorganic polymer cement from ferric and ferrous vitrified residues of plasma gasification. In: Malfliet A, Pontikes Y (eds) Proceedings of 4th international slag valorisation symposium Leuven, pp 319–324
38. Francois E, Elsen J, Pontikes Y, Machiels L (2015) Influence of the chemistry of vitrified residues on the properties of blended inorganic polymers with calcined kaolinitic clay. In: Malfliet A, Pontikes Y (eds) Proceedings of 4th international slag valorisation symposium, Leuven, pp 257–261
39. Arnout L, Machiels L, Cappuyns V, et al (2015) The impact of curing conditions on heavy metal immobilisation of Fe-rich inorganic polymers. In: Malfliet A, Pontikes Y (eds) Proceedings of 4th international slag valorisation symposium, Leuven, pp 249–256
40. Lee NP (2007) Creep and shrinkage of inorganic polymer concrete. BRANZ Study Report SR 175, BRANZ Ltd, Judgeford, New Zealand